

Oxynitride materials for solar water splitting

Kazuhiko Maeda and Kazunari Domen

Water splitting to form hydrogen and oxygen over a heterogeneous photocatalyst using solar energy is a promising process for clean and renewable hydrogen production. In recent years, numerous attempts have been made for the development of photocatalysts that work under visible light irradiation to efficiently utilize solar energy. This article reviews recent research progress in the development of visible light-driven photocatalysts, focusing on the refinement of oxynitride materials. They harvest visible photons (~450–700 nm) and work as stable photocatalysts for water reduction and oxidation under visible light. Oxynitrides with d^0 electronic configuration can be successfully applied to a two-step water-splitting system, which can harvest a wide range of visible photons (~660 nm), in the presence of an iodate/iodide shuttle redox mediator. Also d^{10}-type oxynitrides of GaN–ZnO and $ZnGeN_2$–ZnO solid solutions can achieve functionality as photocatalysts for overall water-splitting under visible light without noticeable degradation.

Introduction

Photocatalytic reactions have been studied extensively in recent years from the viewpoint of environmental accountability and energy conversion. For environmental purposes, TiO_2 with anatase and rutile crystal structures has been predominantly used because of its superior material and economic properties (e.g., chemical stability, non-toxicity, cost-effectiveness).[1,2] In recent research, modified TiO_2 such as N-doped TiO_2 has been examined in order to extend the absorption edge into the visible light region.[3] In application to energy conversion, where research was initially triggered by the potential of TiO_2-based photoelectrochemical (PEC) reactions for the decomposition of water into H_2 and O_2,[4] a range of materials has been examined as powder photocatalysts. These materials include transition metal oxides containing metal ions of Ti^{4+}, Zr^{4+}, Nb^{5+}, Ta^{5+}, or W^{6+} with d^0 electronic configuration and typical metal oxides having metal ions of Ga^{3+}, In^{3+}, Ge^{4+}, Sn^{4+}, or Sb^{5+} with d^{10} electronic configuration.[5–9] Thus, the group of successful photocatalysts for overall water splitting is comprised solely of metal oxide-based systems. Although some non-oxide materials such as CdS and CdSe have been examined, particularly for visible-light catalysis, successful photocatalytic systems have yet to be achieved, primarily due to the lack of oxygen productivity and inherent instability of the materials, which are derived from oxidative self-decomposition of the materials.[10,11]

The two major obstacles to the development of powder photocatalysts are the discovery of new stable photocatalytic materials and the construction of a suitable visible light-driven photocatalytic system. The application of metal oxides for photocatalysis in the visible-light region is complicated by the deep valence band positions (O 2*p* orbitals) of these materials, resulting in a bandgap that is too large to harvest visible light.[12] Since the N 2*p* orbital has a higher potential energy than the O 2*p* orbital, using a metal nitride or metal oxynitride as a photocatalyst has promise. **Figure 1** shows the schematic band structures of a metal oxide ($NaTaO_3$) and oxynitride ($BaTaO_2N$), both of which have the same perovskite structure. The top of the valence band (i.e., highest occupied molecular orbital, HOMO) for the metal oxide consists of O 2*p* orbitals. When N atoms are partially or fully substituted for O atoms in a metal oxide, the HOMO of the material is expected to be shifted higher compared to the corresponding metal oxide without affecting the level of the bottom of the conduction band (i.e., lowest unoccupied molecular orbital, LUMO). As expected, density functional theory (DFT) calculations for $BaTaO_2N$ indicated that the HOMO consists of hybridized N 2*p* and O 2*p* orbitals, whereas the LUMO is mainly composed of empty Ta 5*d* orbitals.[6] The potential of the HOMO for the oxynitride is located at higher potential energy than that for the corresponding oxide due to the contribution of N 2*p* orbitals, making the bandgap energy sufficiently small to respond to visible light (<3 eV). In this article, oxynitrides are presented as non-oxide-type materials for photocatalytic water splitting under visible light.

Kazuhiko Maeda, University of Tokyo, Japan, kmaeda@chemsys.t.u-tokyo.ac.jp
Kazunari Domen, University of Tokyo, Japan, domen@chemsys.t.u-tokyo.ac.jp
DOI: 10.1557/mrs.2010.4

© 2011 Materials Research Society

https://doi.org/10.1557/mrs.2010.4 Published online by Cambridge University Press

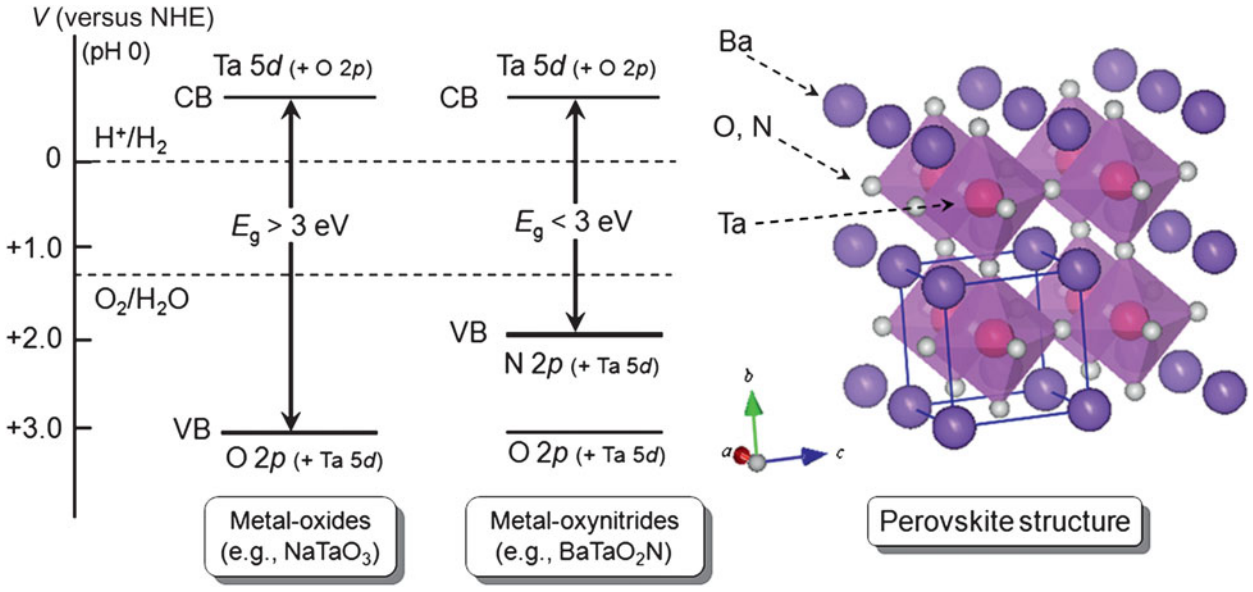


Figure 1. Schematic band structures of a metal oxide ($NaTaO_3$) and metal oxynitride ($BaTaO_2N$) with perovskite structure. The top of the valence band of $BaTaO_2N$ lies at a position less positive than that of $NaTaO_3$, while the conduction band position changes little. CB, conduction band; VB, valence band; E_g, bandgap energy; NHE, normal hydrogen electrode; *V*, potential.

Oxynitrides with d^0 electronic configuration

Preparation and photocatalytic activity

Some particulate oxynitrides containing early transition-metal cations are stable and non-toxic materials and can be readily obtained by nitriding a corresponding metal oxide powder.[13–35] Some metal oxynitrides have recently attracted attention as non-toxic inorganic pigments alternating with chalcogenides-based pigments such as the CdS–CdSe system. For example, a series of $LaTaON_2$–$CaTaO_2N$ solid solutions has been reported to vary in color from yellow to red.[31] In addition, these materials are chemically stable, except in very strong acids, for example, aqua regia and hot concentrated sulfuric acid. Note that this type of material differs from materials doped with nitrogen, because nitrogen is included as a constituent element in oxynitrides. **Figure 2** shows the UV-visible diffuse reflectance spectra for certain oxynitrides containing transition-metal cations of Ti^{4+}, Nb^{5+}, and Ta^{5+} with d^0 electronic configuration. It is clear that these oxynitrides possess absorption bands at 500–750 nm, corresponding to bandgap energies of 1.7–2.5 eV that are estimated from the onset wavelengths of the absorption spectra. As expected from DFT calculations, these oxynitrides have band-edge potentials suitable for overall water splitting, as revealed by UV photoelectron spectroscopy and PEC analysis.[17] For example, it has been revealed that the tops of the valence bands are shifted to higher potential energies in the order Ta_2O_5 < TaON < Ta_3N_5, whereas the potentials of the bottoms of the conduction bands are almost the same.

As overall water splitting is generally difficult to achieve due to the uphill nature of the reaction, photocatalytic activities of a number of oxynitrides for water reduction or oxidation has been examined in the presence of methanol or silver nitrate as a sacrificial reagent. The reactions using sacrificial reagents are not "overall" water splitting reactions, but are often carried out as test reactions for overall water splitting.[6,8] **Table I** lists the photocatalytic activities of d^0-oxynitrides for H_2 or O_2 evolution in the presence of sacrificial reagents. These oxynitrides exhibited relatively high photocatalytic activity for water oxidation to form molecular oxygen under visible irradiation (λ > 420 nm), with some exceptions, such as $ATaO_2N$ (A = Ca, Sr, Ba) and $LaTaON_2$. In contrast, nitrogen-doped TiO_2 displayed negligible activity for this reaction under the same reaction conditions (Table I). Oxynitrides also produced H_2 from an aqueous methanol solution upon visible irradiation when loaded with nanoparticulate Pt as a co-catalyst for H_2 evolution. In most cases, a low level of N_2 evolution accompanied the

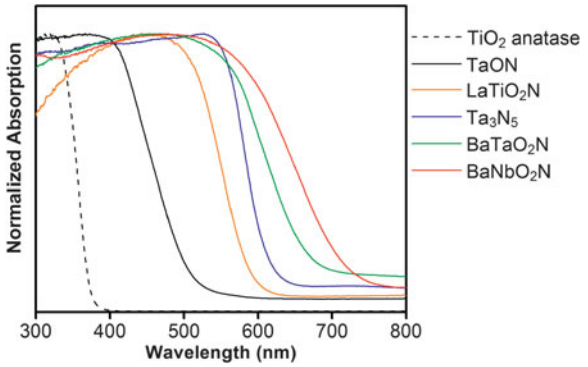


Figure 2. UV-visible diffuse reflectance spectra for oxynitrides containing Ti^{4+}, Nb^{5+}, and Ta^{5+}. It is clear that the oxynitrides have a distinct absorption band in the visible light region.

https://doi.org/10.1557/mrs.2010.4 Published online by Cambridge University Press

Table I. Photocatalytic activities of oxynitrides with d^0 electronic configuration for H_2 or O_2 evolution in the presence of sacrificial reagents under visible light ($\lambda > 420$ nm).[a]

Oxynitride	Bandgap energy[b] (eV)	Activity (μmol h^{-1})		Ref.
		H_2[c]	O_2[d]	
$LaTiO_2N$	2.0	30	41	16
$Ca_{0.25}La_{0.75}TiO_{2.25}N_{0.75}$	2.0	5.5	60	16
$TiN_xO_yF_z$	2.3	0.2	43	18, 20
$CaNbO_2N$	1.9	1.5	46	15
TaON	2.5	20	660	13
Ta_3N_5	2.1	10	420	14
$CaTaO_2N$	2.4	15	0	19
$SrTaO_2N$	2.1	20	0	19
$BaTaO_2N$	1.9	15	0	19
$LaTaON_2$	2.0	20	0	19
N-doped TiO_2	2.6[e]	n.d.	1.6	18, 20

[a]Reaction conditions: 0.2–0.4 g of catalyst, 200 mL aqueous solution containing sacrificial reagents, 300 W xenon lamp light source, Pyrex top irradiation-type reaction vessel with cutoff filter.
[b]Estimated from onset wavelength of diffuse reflectance spectra.
[c]Loaded with nanoparticulate Pt as a co-catalyst, reacted in the presence of methanol (10 vol%), sacrificial reagent.
[d]Sacrificial reagent: silver nitrate (0.01 M).
[e]Energy gap estimated from a shoulder peak (400–500 nm).
n.d., not detected.

initial stage of photocatalytic reactions over these catalysts, indicating that the oxynitride is partially decomposed by the photogenerated holes (instead of water oxidation) according to the reaction:

$$2N^{3-} + 6h^+ \rightarrow N_2. \quad (1)$$

However, the production of N_2 was completely suppressed as the reaction progressed, and no change in the x-ray diffraction pattern of the oxynitrides as a result of the reaction has been detected. It thus appears that oxynitride photocatalysts are essentially stable in the individual water reduction and oxidation reactions.

Improvement of water reduction activity

The activities for H_2 production are about an order of magnitude lower than for O_2 evolution, although the photocatalytic performance for H_2 evolution is stable. In this context, several new modifications to enhance the H_2 evolution rate of oxynitrides have been pursued. Here we introduce such an attempt to reduce the particle size of Ta_3N_5. It is believed that the smaller particle size results in a shorter diffusion length for photogenerated electron–hole-pairs in a given photocatalyst, reducing the recombination between electrons and holes and enhancing photocatalytic activity. We first attempted to increase the photocatalytic activity of TaON for H_2 evolution under visible light by reducing the particle size.[21] However, it was difficult to suppress the generation of defects during the nitridation process, because TaON is an intermediate phase between Ta_2O_5 and Ta_3N_5.[14] As a result, the as-obtained TaON did not show an appreciable increase in photocatalytic activity, despite a relatively small particle size (50–80 nm). In contrast to TaON, preparation of Ta_3N_5 is relatively easy because Ta_3N_5 is the final phase produced by the nitridation of Ta_2O_5.[32,33]

Nanoparticulate Ta_3N_5 can be readily prepared from a nanoparticulate Ta_2O_5 precursor that is synthesized through a precipitation method in advance.[22] Compared to the conventional bulk-type Ta_3N_5 particles (300–500 nm), nanoparticulate Ta_3N_5 with a smaller particle size of 30–50 nm exhibited enhanced photocatalytic activity for H_2 evolution from aqueous solution containing methanol as an electron donor under visible light. Diffuse reflectance spectroscopy and PEC measurements suggested that the enhancement was due to the promotion of the water reduction process originating from the lower defect density of the material.

It is also possible to prepare nano-sized Ta_3N_5 particles through a template approach using a mesoporous graphitic carbon nitride (mpg-C_3N_4),[23] which has a potential to reduce or oxidize water with visible light as well.[36,37] **Figure 3** shows a schematic illustration of the preparation of Ta_3N_5 nanoparticles using mpg-C_3N_4 as a template. Having different pore sizes (7, 12, and 24 nm), mpg-C_3N_4 were prepared by a method similar to one previously reported using colloidal silicas with different particle sizes.[38] The pore space of the as-prepared mpg-C_3N_4 was then filled with a tantalum source such as $TaCl_5$, followed by nitridation under a flow of NH_3 gas. This procedure allows one to prepare Ta_3N_5 nanoparticles with a primary particle size that, in principle, reflects the pore size of mpg-C_3N_4. Interestingly, all Ta_3N_5 nanoparticles thus-obtained showed a much

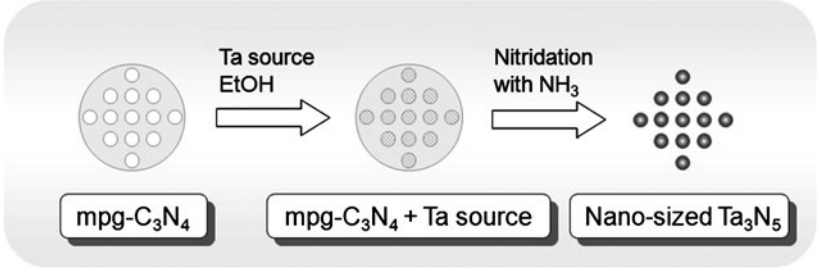


Figure 3. Preparation of Ta_3N_5 nanoparticles using mesoporous graphitic carbon nitride (mpg-C_3N_4) as a template. The pores of mpg-C_3N_4 are filled with Ta source-ethanol (EtOH) solution, followed by nitridation with dry NH_3, yielding Ta_3N_5 nanoparticles.

https://doi.org/10.1557/mrs.2010.4 Published online by Cambridge University Press

higher activity than the reference bulk sample, and Ta_3N_5, having the smallest particle size that was prepared from mpg-C_3N_4 with a pore size of 7 nm, showed approximately one order of magnitude higher activity than bulk Ta_3N_5. In addition to the small particle size and high surface area, the low density of defect sites would also result in an improvement of the activity, since fewer defect sites would be favorable for electron migration from the Ta_3N_5 bulk to the surface and/or electron transfer from the conduction band of Ta_3N_5 to the loaded Pt.[22] This template method may be applicable to other oxynitrides, and this possibility is currently under investigation.

As mentioned earlier, it seems difficult to control the crystallinity of TaON by adjustment of preparation parameters alone because TaON is an intermediate phase between Ta_2O_5 and Ta_3N_5.[14] Although the calcination of solid photocatalysts after preparation has been demonstrated to be an effective approach for reducing the density of defects,[39,40] such post-calcination appears to be disadvantageous for TaON due to its low thermal stability. In fact, post-calcination of TaON under O_2 or N_2 results in a decrease in activity.[41] The elimination of defects in TaON therefore remains a challenge.

Recently, we have developed a new strategy to reduce surface defects on TaON using ZrO_2 as a "protector" through a surface modification technique.[24,25] Specifically, monoclinic ZrO_2 nanoparticles are dispersed on the surface of a Ta_2O_5 precursor before nitridation, thereby protecting Ta^{5+} cations in the TaON surface from being reduced by H_2 (derived from disassociation of NH_3 at high temperatures) during nitridation. As has been observed for other oxynitrides such as $LaTiO_2N$[16] and $TiN_xO_yF_z$,[20] the reduction of Ta^{5+} cations in TaON during nitridation generates reduced tantalum species, which can act as recombination centers between photogenerated electrons and holes. On the other hand, when ZrO_2 is loaded on the surface of Ta_2O_5, tantalum cations at the interface between Ta_2O_5 (and/or TaON) and the loaded ZrO_2 are expected to interact with ZrO_2 and thereby become more cationic. As a result, the formation of reduced tantalum species on the TaON surface is effectively suppressed by prior loading with nanoparticulate ZrO_2. As expected, the as-prepared ZrO_2-modified TaON (represented as ZrO_2/TaON) exhibited enhanced water reduction behavior compared to unmodified TaON. This enhancement of activity is attributed to the reduced density of defects in ZrO_2/TaON, which contributes to a lower probability of undesirable electron–hole recombination in ZrO_2/TaON than in TaON.

Despite the efforts mentioned previously, overall water splitting using these d^0-oxynitrides has yet to be achieved. One plausible explanation for this is that they still have a high density of defect sites that can work as recombination centers for photogenerated electrons and holes. Nevertheless, z-scheme overall water splitting under visible light has been achieved using several combinations of oxynitrides in the presence of an IO_3^-/I^- shuttle redox mediator, as schematically illustrated in **Figure 4**.[24–29] The use of Pt-loaded $BaTaO_2N$ allows one to utilize visible photons up to 660 nm for H_2 evolution when combined with Pt-loaded WO_3, which has an absorption edge at around 450 nm, as an O_2 evolution photocatalyst.[27] The absorption wavelength available for O_2 evolution was then increased to 500 nm using RuO_2-loaded TaON[28] and to 600 nm using Ir-loaded nanoparticulate TiO_2 (rutile)/bulk Ta_3N_5 composite.[29] Thus, the absorption wavelength available for the individual H_2 and O_2 evolution has been increased. The next challenges remain in the promotion of electron transfer between two semiconductors and in the suppression of backward reactions involving shuttle redox mediators.

Another application has been reported for d^0-oxynitrides working as anode materials for photoelectrochemical water splitting under visible light.[41–44] In this approach, not only light energy but also electric energy can be put into the system for operation, resulting in a relatively high incident photon-to-current conversion efficiency (IPCE), with stoichiometric H_2 and O_2 evolution.[44] However, suppressing the oxidative self-decomposition by the valence band holes (Reaction 1) to stabilize the system during photoelectrolysis still remains a challenge.

Oxynitrides with d^{10} electronic configuration

Difference in electronic band structure between d^0- and d^{10}-based photocatalysts

Until 2005, oxynitride photocatalysts having the ability to reduce and/or oxidize water under visible light had been composed of transition-metal cations of Ti^{4+}, Nb^{5+}, or Ta^{5+} with d^0 electronic configuration.[13–19] From the viewpoint of the electronic band

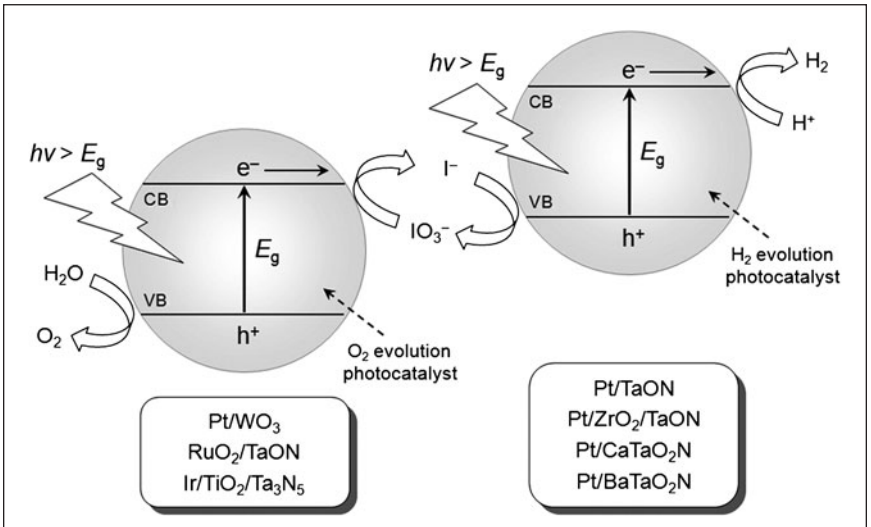


Figure 4. A schematic illustration of a two-step water-splitting system based on oxynitrides in the presence of an iodate/iodide shuttle redox mediator. Water reduction occurs on a H_2 evolution photocatalyst, while an O_2 evolution photocatalyst plays a role in oxidizing water. Electron transfer between the two photocatalysts is mediated by an IO_3^-/I^- shuttle redox mediator. CB, conduction band; VB, valence band; *h*, Planck's constant; ν, frequency; E_g, bandgap energy.

https://doi.org/10.1557/mrs.2010.4 Published online by Cambridge University Press

structure, however, d^{10}-based semiconducting materials are advantageous over the d^0 configurations as a photocatalyst in that while the top of the valence band consists of O 2*p* orbitals, the bottom of the conduction band is composed of hybridized *sp* orbitals of typical metals.[9] The hybridized *sp* orbitals possess large dispersion, leading to increased mobility of photogenerated electrons in the conduction band and thus high photocatalytic activity. This has stimulated study on oxynitrides, with the d^{10} electronic configuration as a photocatalyst for overall water splitting.

Oxynitrides with a d^{10} electronic configuration are therefore of interest as potentially efficient photocatalysts for overall water splitting. In evaluating such d^{10}-compounds according to this hypothesis, it was found that β-Ge_3N_4 loaded with RuO_2 nanoparticles functions as a photocatalyst for overall water splitting.[45–48] This was the first case involving a non-oxide photocatalyst for the cleavage of pure water. Since this discovery, the photocatalytic properties and effects of post-treatment to enhance the activity of Ge_3N_4 have been examined in detail.[46,47] The relationship between the structural characteristics and the photocatalytic performance of Ge_3N_4 has also been investigated.[48] Unfortunately, the bandgap of β-Ge_3N_4 is about 3.8 eV, which is responsive only to ultraviolet light.[45,47] This forced us to search for a new d^{10} compound that can function under visible light.

GaN–ZnO solid solution

To devise a new oxynitride with d^{10} electronic configuration that can decompose water under visible light, the solid solution of GaN and ZnO $(Ga_{1-x}Zn_x)(N_{1-x}O_x)$ was examined.[49,50] The detailed concept for designing the material as a visible-light-driven photocatalyst has been described elsewhere.[51] The $(Ga_{1-x}Zn_x)(N_{1-x}O_x)$ solid solution is typically synthesized by nitriding a mixture of Ga_2O_3 and ZnO. Elemental analyses by inductively coupled plasma optical emission spectroscopy (ICP-OES) revealed that the ratios of Ga to N and Zn to O in the as-prepared material are close to unity, and N and O concentrations increase with the Ga and Zn concentrations, respectively.[49] The atomic composition is controllable by changing the nitridation conditions.[51] X-ray diffraction and neutron powder diffraction analyses showed that the prepared samples are solid solutions of GaN and ZnO with no interstitial sites and no large disorder in the material.[49,50,52] While GaN and ZnO both have bandgap energies greater than 3 eV and thus do not absorb visible light, the $(Ga_{1-x}Zn_x)(N_{1-x}O_x)$ solid solution has absorption edges in the visible region. **Figure 5** shows the UV-visible diffuse reflectance spectra for several samples. The absorption edge of $(Ga_{1-x}Zn_x)(N_{1-x}O_x)$ lies at a wavelength longer than those of GaN and ZnO and shifts to longer wavelengths with increasing Zn and O concentration (*x*) in $(Ga_{1-x}Zn_x)(N_{1-x}O_x)$. The bandgap energies of the solid solutions are estimated to be 2.4–2.8 eV based on the diffuse reflectance spectra. It is thus clear that the visible-light-response of $(Ga_{1-x}Zn_x)(N_{1-x}O_x)$ originates from the presence of ZnO in the crystal. The photoluminescence and photoluminescence excitation spectra of $(Ga_{1-x}Zn_x)(N_{1-x}O_x)$ with compositions of

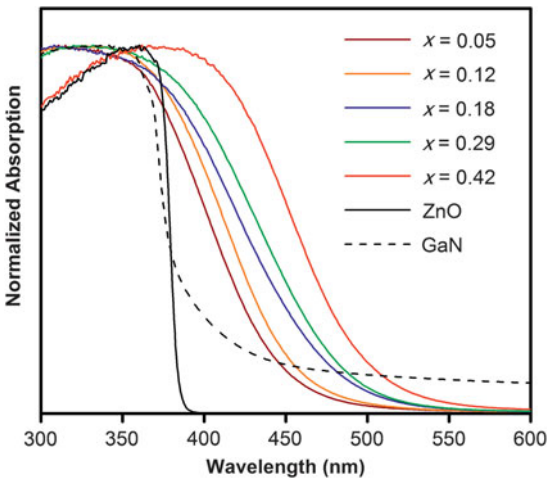


Figure 5. UV-visible diffuse reflectance spectra for various $(Ga_{1-x}Zn_x)(N_{1-x}O_x)$ solid solutions. The position of the absorption edge of $(Ga_{1-x}Zn_x)(N_{1-x}O_x)$ is located at a wavelength longer than that of GaN and ZnO and is shifted to longer wavelengths with increasing Zn and O concentration.

$x = 0.05–0.20$ (i.e., GaN-rich) measured at 10 K suggested that the visible light absorption of this material occurs via Zn-related acceptor levels.[53] This idea, however, contradicts our early DFT calculations, which indicate that the bottom of the conduction band for $(Ga_{1-x}Zn_x)(N_{1-x}O_x)$ is mainly composed of 4*s* and 4*p* orbitals of Ga, while the top of the valence band consists of N 2*p* orbitals followed by Zn 3*d* and O 2*p* orbitals.[49,50] This idea remains valid for the solid solution with stoichiometric unit cells. For a dilute solid solution, however, it is natural to consider the local inhomogeneity of the Zn and O atom densities. In such circumstances, empty impurity levels appear just above the valence band, and/or filled impurity levels appear just below the conduction band. These impurity levels may explain the present experimental results and were characterized by DFT calculations with nonstoichiometric unit cells. Very recently, Muckerman et al. and Huang et al. have studied the same material using theoretical calculations.[54,55] Their results are essentially identical to those obtained in our previous study.

The as-prepared $(Ga_{1-x}Zn_x)(N_{1-x}O_x)$ exhibited little photocatalytic activity for water decomposition even under UV irradiation. However, modification by surface deposition of metal oxide nanoparticles (so-called co-catalysts), such as H_2 evolution sites, resulted in clearly observable H_2 and O_2 evolution. The activity was strongly dependent on the loaded co-catalyst, and a mixed-oxide of Rh and Cr $(Rh_{2-y}Cr_yO_3)$ is the most effective $(Ga_{1-x}Zn_x)(N_{1-x}O_x)$ among the co-catalyst materials examined.[56,57] **Figure 6** displays a typical time course of visible-light-driven overall water splitting over $Rh_{2-y}Cr_yO_3$-loaded $(Ga_{1-x}Zn_x)(N_{1-x}O_x)$. As can be seen, this photocatalyst produced both H_2 and O_2 in the stoichiometric ratio $(H_2/O_2 = 2)$ without noticeable degradation. The photocatalytic performance was also dependent on the pH of the reactant solution.[58] The photocatalyst

https://doi.org/10.1557/mrs.2010.4 Published online by Cambridge University Press

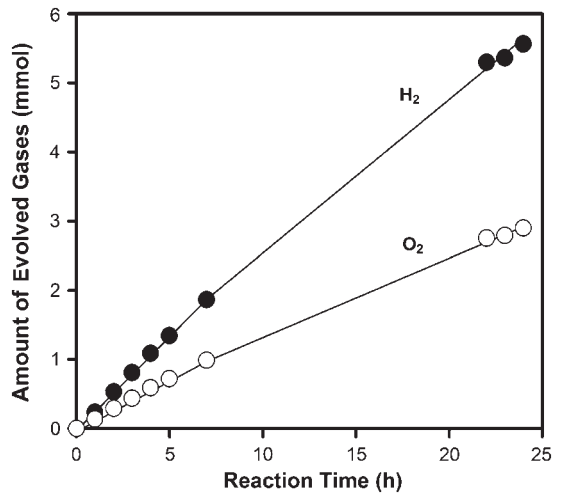


Figure 6. A typical time course of overall water splitting under visible irradiation (wavelength, $\lambda > 400$ nm) over $Rh_{2-y}Cr_yO_3$-loaded $(Ga_{1-x}Zn_x)(N_{1-x}O_x)$ (1.0 wt% Rh and 1.5 wt% Cr). Here it is clear that the photocatalyst catalyzes stoichiometric water splitting into H_2 and O_2 with visible light. Catalyst (0.3 g); reactant solution, aqueous H_2SO_4 solution (370 mL, pH 4.5); light source, high-pressure mercury lamp (450 W) with an aqueous $NaNO_2$ solution (2 M) filter; inner-irradiation-type Pyrex reaction vessel.

exhibited stable and high photocatalytic activity in an aqueous solution at pH 4.5 for as long as three days. The photocatalytic performance at pH 3.0 and pH 6.2 was much lower, attributable to corrosion of the co-catalyst and hydrolysis of the catalyst. It has also been confirmed by x-ray diffraction, x-ray photoelectron spectroscopy, and x-ray absorption fine structure that the crystal structure of the catalyst and the valence state of both the surface and bulk do not change even after reaction for three days at optimal pH (4.5). These results offer useful guidelines for further research using other oxynitrides.

$ZnGeN_2$–ZnO solid solution

A solid solution of $ZnGeN_2$ and ZnO, $(Zn_{1+x}Ge)(N_2O_x)$, which is a similar material to $(Ga_{1-x}Zn_x)(N_{1-x}O_x)$ in terms of crystal structure and optical absorption, has also been found to be an active and stable photocatalyst for overall water splitting under visible light.[59,60] Both $ZnGeN_2$ and ZnO are wide-gap semiconductors with bandgaps larger than 3 eV, although the bandgap of $ZnGeN_2$ is dependent on the crystal structure and composition.[61] The $(Zn_{1+x}Ge)(N_2O_x)$ solid solutions can be prepared in a method similar to $(Ga_{1-x}Zn_x)(N_{1-x}O_x)$, but with a mixture of ZnO and GeO_2 as the starting material. The crystal structure of the synthesized sample was confirmed by both Rietveld analysis and neutron powder diffraction to be wurtzite with space group $P6_3mc$.[59] In the solid solution between $ZnGeN_2$ and ZnO, the oxygen atoms are replaced with nitrogen sites. The bandgap of the material is estimated to be 2.5–2.7 eV based on the absorption edges, which is smaller than the bandgaps of β-Ge_3N_4 (ca. 3.8 eV), $ZnGeN_2$ (ca. 3.3 eV), and ZnO (ca. 3.2 eV). The visible-light response of the material originates from the wide valence bands consisting of N 2*p*, O 2*p*, and Zn 3*d* atomic orbitals and *p*–*d* repulsion between Zn 3*d* and N 2*p* and O 2*p* electrons in the upper part of the valence bands. Therefore, the absorption edge of $(Zn_{1+x}Ge)(N_2O_x)$ tends to be located at longer wavelengths with increasing ZnO content.

Neither $ZnGeN_2$ nor ZnO alone exhibited photocatalytic activity for overall water splitting under UV irradiation. However, $(Zn_{1+x}Ge)(N_2O_x)$ became photocatalytically active under visible irradiation when loaded with a proper co-catalyst. Overall water splitting on a modified $(Zn_{1+x}Ge)(N_2O_x)$ proceeded by bandgap photoexcitation from the valence band formed by N 2*p*, O 2*p*, and Zn 3*d* atomic orbitals to the conduction band consisting of Ge 4*s*,4*p* hybridized atomic orbitals. As demonstrated in the $(Ga_{1-x}Zn_x)(N_{1-x}O_x)$ section earlier, the photocatalytic activity of the transition metal-loaded catalysts was improved markedly by co-loading Cr oxide.[60] The largest improvement in activity was obtained by loading the base catalysts with both 3 wt% Rh and 0.2 wt% Cr. It was confirmed that catalytic gas evolution of $Rh_{2-y}Cr_yO_3$-loaded $(Zn_{1+x}Ge)(N_2O_x)$ is stable for as long as 60 h.

Summary

A range of oxynitride materials for photocatalytic overall water splitting has been developed. Oxynitrides have been found to function as stable photocatalysts for water reduction and oxidation under visible irradiation, and the $(Ga_{1-x}Zn_x)(N_{1-x}O_x)$ and $(Zn_{1+x}Ge)(N_2O_x)$ solid solutions with d^{10} electronic configuration have been shown to achieve overall water splitting under visible light without noticeable degradation. Some of d^0-type oxynitrides are applicable to a two-step water splitting system that can harvest a wide range of visible photons. Although the quantum yield of photocatalytic water splitting still remains ~5–6% in this research field, further research on materials chemistry in oxynitrides is expected to improve the performance.

Acknowledgments

The research described herein was supported by the 21st Century Center of Excellence (COE) and the Research and Development in a New Interdisciplinary Field Based on Nanotechnology and Materials Science programs of the Ministry of Education, Culture, Sports, Science and Technology (MEXT) of Japan. Acknowledgment is also extended to the KAITEKI Institute, Inc. for financial support. Acknowledgment is also extended to the Global Center of Excellence (GCOE) Program for Chemistry Innovation through Cooperation of Science and Engineering and Nippon Sheet Glass Foundation for Materials Science and Engineering.

References

1. M.R. Hoffmann, S.T. Martin, W.Y. Choi, D.W. Bahnemann, *Chem. Rev.* **95**, 69 (1995).
2. A. Fujishima, T.N. Rao, D.A. Tryk, *J. Photochem. Photobiol. C* **1**, 1 (2000).
3. R. Asahi, T. Morikawa, T. Ohwaki, K. Aoki, Y. Taga, *Science* **293**, 269 (2001).
4. A. Fujishima, K. Honda, *Nature* **238**, 37 (1972).
5. K. Domen, J.N. Kondo, M. Hara, T. Takata, *Bull. Chem. Soc. Jpn.* **73**, 1307 (2000).
6. K. Maeda, K. Domen, *J. Phys. Chem. C* **111**, 7851 (2007).

https://doi.org/10.1557/mrs.2010.4 Published online by Cambridge University Press

7. F.E. Osterloh, *Chem. Mater.* **20**, 35 (2008).
8. A. Kudo, Y. Miseki, *Chem. Soc. Rev.* **38**, 253 (2009).
9. Y. Inoue, *Energy Environ. Sci.* **2**, 364 (2009).
10. R. Williams, *J. Chem. Phys.* **32**, 1505 (1960).
11. A.B. Ellis, S.W. Kaiser, J.M. Bolts, M.S. Wrighton, *J. Am. Chem. Soc.* **99**, 2839 (1977).
12. D.E. Scaife, *Solar Energy* **25**, 41 (1980).
13. G. Hitoki, T. Takata, J.N. Kondo, M. Hara, H. Kobayashi, K. Domen, *Chem. Commun.* 1698 (2002).
14. G. Hitoki, A. Ishikawa, T. Takata, J.N. Kondo, M. Hara, K. Domen, *Chem. Lett.* **31**, 736 (2002).
15. G. Hitoki, T. Takata, J.N. Kondo, M. Hara, H. Kobayashi, K. Domen, *Electrochem.* **70**, 463 (2002).
16. A. Kasahara, K. Nukumizu, G. Hitoki, T. Takata, J.N. Kondo, M. Hara, H. Kobayashi, K. Domen, *J. Phys. Chem. A* **106**, 6750 (2002).
17. W.-A. Chun, A. Ishikawa, H. Fujisawa, T. Takata, J.N. Kondo, M. Hara, M. Kawai, Y. Matsumoto, K. Domen, *J. Phys. Chem. B* **107**, 1798 (2003).
18. K. Nukumizu, J. Nunoshige, T. Takata, J.N. Kondo, M. Hara, H. Kobayashi, K. Domen, *Chem. Lett.* **32**, 196 (2003).
19. D. Yamasita, T. Takata, M. Hara, J.N. Kondo, K. Domen, *Solid State Ionics* **172**, 591 (2004).
20. K. Maeda, Y. Shimodaira, B. Lee, K. Teramura, D. Lu, H. Kobayashi, K. Domen, *J. Phys. Chem. C* **111**, 18264 (2007).
21. K. Maeda, H. Terashima, K. Kase, K. Domen, *Appl. Catal., A* **357**, 206 (2009).
22. K. Maeda, N. Nishimura, K. Domen, *Appl. Catal., A* **370**, 88 (2009).
23. L. Yuliati, J.-H. Yang, X. Wang, K. Maeda, T. Takata, M. Antonietti, K. Domen, *J. Mater. Chem.* **20**, 4295 (2010).
24. K. Maeda, H. Terashima, K. Kase, M. Higashi, M. Tabata, K. Domen, *Bull. Chem. Soc. Jpn.* **81**, 927 (2008).
25. K. Maeda, M. Higashi, D. Lu, R. Abe, K. Domen, *J. Am. Chem. Soc.* **132**, 5858 (2010).
26. R. Abe, T. Takata, H. Sugihara, K. Domen, *Chem. Commun.* 3829 (2005).
27. M. Higashi, R. Abe, K. Teramura, T. Takata, B. Ohtani, K. Domen, *Chem. Phys. Lett.* **452**, 120 (2008).
28. M. Higashi, R. Abe, A. Ishikawa, T. Takata, B. Ohtani, K. Domen, *Chem. Lett.* **37**, 138 (2008).
29. M. Tabata, K. Maeda, M. Higashi, D. Lu, T. Takata, R. Abe, K. Domen, *Langmuir* **26**, 9161 (2010).
30. F. Tessier, R. Marchand, *J. Alloys Compd.* **262–263**, 410 (1997).
31. M. Jansen, H.P. Letschert, *Nature* **404**, 980 (2000).
32. R. Marchand, F. Tessiera, F.J. DiSalvob, *J. Mater. Chem.* **9**, 297 (1999).
33. Q. Zhang, L. Gao, *Langmuir* **20**, 9821 (2004).
34. S. Ito, K.R. Thampi, P. Comte, P. Liska, M. Grätzel, *Chem. Commun.* 268 (2005).
35. T. Mishima, M. Matsuda, M. Miyake, *Appl. Catal., A* **324**, 77 (2007).
36. X. Wang, K. Maeda, A. Thomas, K. Takanabe, G. Xin, J.M. Carlsson, K. Domen, M. Antonietti, *Nat. Mater.* **8**, 76 (2009).
37. X. Wang, K. Maeda, X. Chen, K. Takanabe, K. Domen, Y. Hou, X. Fu, M. Antonietti, *J. Am. Chem. Soc.* **131**, 1680 (2009).
38. F. Goettmann, A. Fischer, M. Antonietti, A. Thomas, *Angew. Chem., Int. Ed.* **45**, 4467 (2006).
39. K. Sayama, H. Arakawa, K. Domen, *Catal. Today* **28**, 175 (1996).
40. H. Kominami, S. Murakami, Y. Kera, B. Ohtani, *Catal. Lett.* **56**, 125 (1998).
41. R. Abe, T. Takata, H. Sugihara, K. Domen, *Chem. Lett.* **34**, 1162 (2005).
42. R. Nakamura, T. Tanaka, Y. Nakato, *J. Phys. Chem. B* **109**, 8920 (2005).
43. X. Feng, T.J. LaTempa, J.I. Basham, G.K. Mor, O.K. Varghese, C.A. Grimes, *Nano Lett.* **10**, 948 (2010).
44. R. Abe, M. Higashi, K. Domen, *J. Am. Chem. Soc.* **132**, 11828 (2010).
45. J. Sato, N. Saito, Y. Yamada, K. Maeda, T. Takata, J.N. Kondo, M. Hara, H. Kobayashi, K. Domen, Y. Inoue, *J. Am. Chem. Soc.* **127**, 4150 (2005).
46. Y. Lee, T. Watanabe, T. Takata, M. Hara, M. Yoshimura, K. Domen, *J. Phys. Chem. B* **110**, 17563 (2006).
47. K. Maeda, N. Saito, D. Lu, Y. Inoue, K. Domen, *J. Phys. Chem. C* **111**, 4749 (2007).
48. K. Maeda, N. Saito, Y. Inoue, K. Domen, *Chem. Mater.* **19**, 4092 (2007).
49. K. Maeda, T. Takata, M. Hara, N. Saito, Y. Inoue, H. Kobayashi, K. Domen, *J. Am. Chem. Soc.* **127**, 8286 (2005).
50. K. Maeda, K. Teramura, T. Takata, M. Hara, N. Saito, K. Toda, Y. Inoue, H. Kobayashi, K. Domen, *J. Phys. Chem. B* **109**, 20504 (2005).
51. K. Maeda, K. Domen, *Chem. Mater.* **22**, 612 (2010).
52. M. Yashima, K. Maeda, K. Teramura, T. Takata, K. Domen, *Chem. Phys. Lett.* **416**, 225 (2005).
53. T. Hirai, K. Maeda, M. Yoshida, J. Kubota, S. Ikeda, M. Matsumura, K. Domen, *J. Phys. Chem. C* **111**, 18853 (2007).
54. L.L. Jensen, J.T. Muckerman, M.D. Newton, *J. Phys. Chem. C* **112**, 3439 (2008).
55. W. Wei, Y. Dai, K. Yang, M. Guo, B. Huang, *J. Phys. Chem. C* **112**, 15915 (2008).
56. K. Maeda, K. Teramura, D. Lu, T. Takata, N. Saito, Y. Inoue, K. Domen, *Nature* **440**, 295 (2006).
57. K. Maeda, K. Teramura, N. Saito, Y. Inoue, K. Domen, *J. Catal.* **243**, 303 (2006).
58. K. Maeda, K. Teramura, H. Masuda, T. Takata, N. Saito, Y. Inoue, K. Domen, *J. Phys. Chem. B* **110**, 13107 (2006).
59. Y. Lee, H. Terashima, Y. Shimodaira, K. Teramura, M. Hara, H. Kobayashi, K. Domen, M. Yashima, *J. Phys. Chem. C* **111**, 1042 (2007).
60. Y. Lee, K. Teramura, M. Hara, K. Domen, *Chem. Mater.* **19**, 2120 (2007).
61. T. Misaki, X. Wu, A. Wakahara, A. Yoshida, *Proc. Int. Workshop Nitride Semiconductors IPAP Conf. Series 1* 685 (2000). □

7TH INTERNATIONAL
DENDRIMER
SYMPOSIUM

National Institute for
Standards and Technology (NIST)
Gaithersburg, Maryland, USA

www.mrs.org/IDS7

7th International Dendrimer Symposium • June 26–July 1, 2011

BACKGROUND
Dendrimers are monodisperse polymeric materials with branched architecture, first reported as cascade molecules by Professor Fritz Vögtle in 1978 and later reported by Dr. Donald Tomalia and Professor George Newkome in 1985 as dendrimers and arborols, respectively. The field has expanded in the past 25 years and now dendrimers, dendritic polymers and hyperbranched architectures have found application in various fields including materials, catalysis, defense, energy, environmental remediation and biomedical applications, to name a few.

INTRODUCTION
With the exponential growth of this field, and with many groups pursuing dendrimer research all over the globe, researchers felt the need for a dedicated international symposium to bring multidisciplinary groups working with dendrimers together to discuss their research. As a result, the first international dendrimer symposium was organized in Frankfurt, Germany (1999) followed every two years by Tokyo, Japan (2001); Berlin, Germany (2003); Mt. Pleasant, MI, USA (2005); Toulouse, France (2007); and Stockholm, Sweden (2009). An average of 300-400 participants from over 30 countries attended each of these symposia.

FOCUS
This symposium will focus on the latest developments in technology, synthesis, characterization and applications. The meeting format will offer limited parallel sessions with sufficient breaks and social gatherings to provide for collaborative networking opportunities, including a welcome reception, poster sessions, coffee breaks and a conference dinner.

For additional information, please contact:
Dr. Anil K. Patri
Deputy Director
Nanotechnology Characterization Laboratory
Email: patria@mail.nih.gov
Phone: 301.846.5237

The 7th International Dendrimer Symposium will be managed by the Materials Research Society. MRS

https://doi.org/10.1557/mrs.2010.4 Published online by Cambridge University Press